NASA Technical Memorandum 105799

Effects of Anode Material on Arcjet Performance

John M. Sankovic and Frank M. Curran
Lewis Research Center
Cleveland, Ohio

and

C.A. Larson
United States Air Force Academy
Colorado Springs, Colorado

Prepared for the
1992 JANNAF Propulsion Meeting
Indianapolis, Indiana, February 24–28, 1992

EFFECTS OF ANODE MATERIAL ON ARCJET PERFORMANCE

J. M. Sankovic* and F. M. Curran**
National Aeronautics and Space Administration
Lewis Research Center
Cleveland, Ohio 44135-3191

and

C. A. Larson†
United States Air Force Academy
Colorado Springs, Colorado 80840-5701

ABSTRACT

Anodes fabricated from four different materials were tested in a modular arcjet thruster at the 1 kW power level on nitrogen/hydrogen mixtures. A two-percent thoriated tungsten anode served as the control. Graphite was chosen for its ease in fabrication, but experienced severe erosion in the constrictor and diverging side. Hafnium carbide and lanthanum hexaboride were chosen for their low work functions but failed due to thermal stress and reacted with the propellant. When compared to the thoriated tungsten nozzle, thruster performance was significantly lower for the lanthanum hexaboride insert and the graphite nozzle, but was slightly higher for the hafnium carbide nozzle. Both the lanthanum hexaboride and hafnium carbide nozzle operated at higher voltages. An attempt was made to duplicate higher performance hafnium carbide results, but repeated attempts at machining a second anode insert were unsuccessful. Graphite, hafnium carbide, and lanthanum hexaboride do not appear viable anode materials for low power arcjet thrusters.

INTRODUCTION

The arcjet thruster operates on the simple concept of using an electric arc to heat the propellant instead of a chemical reaction. The anode also serves as a supersonic nozzle to convert the thermal energy into directed kinetic energy and thereby produce thrust. A large amount of research was conducted in the late 1950's and continued until the mid-1960's. That research concentrated on using arcjets for primary propulsion applications at the 30 kW power level with hydrogen as the propellant[1,2]. A limited amount of work was also done at 1-2 kW power level. A 150 hour endurance test was successfully completed at 2 kW on hydrogen, but long life and stability were never achieved during that research effort[3,4]. Lack of lightweight space power sources and power processors brought an end to arcjet research in the mid 1960's. An excellent summary of the arcjet effort during that time period is provided by Wallner and Czika[5].

During the mid-1980's research in the arcjet was rekindled with the need for high specific impulse. The idea was to use existing storable propellant technology with a new propulsion system. The design philosophy included the development of an arcjet system including the thruster, power conditioning unit (PCU), and gas generator. Low power thruster life and stability were demonstrated by Curran and Haag[6] in a 1000 hour/ 500 cycle endurance test on simulated fully decomposed hydrazine in 1987. Currently, a 1.8 kW hydrazine arcjet system with a 91-94% efficient PCU, and a thruster capable of providing a specific impulse of 520 s at an efficiency of 0.35 is undergoing flight qualification.[7] The system is baselined on a commerical communications satellite series for north-south stationkeeping with the first mission scheduled for launch in late 1993. Work is also underway in high power arcjets for orbit raising missions. Performance has recently been measured on a hydrogen arcjet at 5-30 kW with three different nozzle geometries under a jointly sponsored NASA/SDIO program[8]. Under that same program, a 10 kW PCU has been designed and successfully tested with a hydrogen arcjet as the load[9]. The Air Force is developing the 30 kW class Advanced Technology Transition Demonstration effort with the objective of developing and demonstrating on the ground a flight qualified arcjet propulsion unit using ammonia as the propellant. Once flight qualification is complete the unit will be space tested in the Electric Propulsion Space Experiment (ESEX) planned for launch in 1995. Also, the Air Force is continuing with the Electric Insertion Transfer Experiment (ELITE) as a precursor to an operational electric orbit transfer vehicle (EOTV). The objective of ELITE is to demonstrate a fully integrated EOTV in a representative mission scenerio[10]. In support of these efforts the Jet Propulsion Laboratory (JPL) has recently completed a 1460 hour endurance test of an ammonia arcjet at 10 kW with electrode erosion not being the factor in test termination[11,12].

The electrodes are a critical area in all arcjet thrusters. Both the anode and cathode are subjected to extremely high heat fluxes, and prevention of electrode dimension distortion is critical. Since the anode also serves as the nozzle, erosion can cause stability and performance issues. Work has already been performed on using various materials for arcjet cathodes.

---

* Aerospace engineer, Low Thrust Propulsion Branch
** Senior Research Scientist, Low Thrust Propulsion Branch
† 1991 USAF Cadet Summer Research Program

Hardy and Curran[13] investigated the use of hollow cathodes for arcjet applications, and Curran *et al.*[14] tested 2% ThO_2/W, 4% ThO_2/W, 2% ThO_2/25% Re/W, 2% ThO_2/Re, and HfC as cathode materials. The outcome of those tests showed 2% ThO_2/W to be the material of choice. Testing of anode materials for arcjets has been limited to refractory metals and graphite with emphasis on erosion and chemical compatibility with the propellant. Graphite nozzles were tested during the Plasmadyne 1 kW arcjet program in the early 1960's on hydrogen[15]. The results of those tests showed that graphite and tungsten coated graphite were not suitable anode material due to severe erosion. However, long lifetimes at the 1 kW power level were never achieved during that decade, and the starting technique frequently caused nozzle damage which may have significantly contributed to the the erosion noted[16]. Rocket Research Company (RRC) tested the compatibility of catalytically decomposed hydrazine with W, W/25% Re, Mo/41% Re and Re. The rhenium alloys were chosen because of their previously demonstrated resistance to oxidation in resistojets. The results of the testing showed no evidence to support selecting any materials other than pure tungsten which had the lowest start-up erosion.[17]

The main goal of present low power arcjet effort is to increase performance while maintaining life. Theoretically, arcjet efficiency could be increased by decreasing the anode losses which consists of radiation, convection, and the contribution from the electron current[18]. The electron current term is comprised of the energy the electrons possess due to their temperature at the edge of the anode fall region, the energy they gain passing through the anode fall, and the energy gained by entering the anode surface. The energy the electrons release when entering the anode surface is a function of the work function of the material. Since the amount of energy lost to the anode depends on the work function, it is hoped that by lowering the work function more energy will be available for thrust.

This study investigated arcjet performance and the viability of four materials as arcjet anodes. The materials included 2% thoriated tungsten, hafnium carbide, lanthanum hexaboride, and graphite. Tungsten and thoriated tungsten have been used as arcjet anode materials for the past thirty years. Pure tungsten has a work function of 4.5 eV while adding 2% ThO_2 will reduce the work function to that of thoria, 3.3 eV[19]. The addition of the thoria also increases the machinability of the anode, but complicates integration of the anode to a flight representative thruster body because of electron beam welding difficulty. Due to the ease of fabrication, and past successes with thoriated tungsten anode inserts at NASA Lewis[6], a 2% ThO_2 anode was used as the control. Hafnium carbide appeared to have the most promise of the carbide materials as an arcjet anode due to its low work function of 2.0-4.0 eV[20] and its high melting point of 3890 °C[21]. Likewise lanthanum hexaboride with a work function of 2.7 eV[20], a melting point of 2530°C[22], and metallic thermal conductivity appeared the most favorable material from the boride family. The fourth material tested was graphite. Although graphite with a work function of 4.4 eV[20] has no work function advantages over 2% ThO_2 , its inexpensive material and fabrication costs would make it a excellent candidate for parametric nozzle tests, and it was hoped that the high erosion rates noted by Plasmadyne were a result of their harsh starting techniques. Performance tests were conducted at the 1 kW power level using 2% thoriated tungsten, hafnium carbide, lanthanum hexaboride, and graphite as the anode inserts. All tests were conducted using a mixture of nitrogen and hydrogen to simulate fully decomposed hydrazine. The performance data were compared, revealing differences in current/voltage characteristics, efficiency, and specific impulse. Scanning electron micrographs were taken before and after testing to reveal nozzle erosion. Using those data, the viability of each material for use in arcjet anodes was determined.

EXPERIMENTAL APPARATUS

ANODES

Anode inserts of the type used in previous low power arcjet testing[23] were used. All four of the anodes were fabricated to the same dimensions. The converging side had a 30° half angle to match the cathode and the diverging side had a half angle of 20°. The constrictor diameter was 0.064 cm in diameter and had a length of 0.025 cm. The nozzle area ratio was 225. All nozzles were fabricated on a lathe using carbide machine tools. Machining of the hafnium carbide nozzle was extremely difficult due to the materials brittleness, and attempts to fabricate a second anode in order to repeat data were unsuccessful. Also, hafnium carbide at elevated temperatures will react with atmospheric oxygen, a problem which posed difficulty during machining of the anode.

ARCJET THRUSTER

The arcjet thruster used was the low power, modular design developed at NASA Lewis[23]. A schematic of the thruster with the anode insert is shown in Figure 1. The cathode consisted of a 0.318 cm diameter, 2% ThO_2/W rod with a 30° half angle conical tip. The anodes fit into a titaniated-zirconiated-molybdenum (TZM) housing. The front insulator consisted of high purity boron nitride, while the rear insulator contained a calcium oxide binder. The propellant injection disk was also fabricated from TZM. The propellant injection was through two 0.051 cm diameter holes perpendicular to the cathode and constrictor. Sealing surfaces utilized gaphite foil gaskets. The arc gap was set by touching the electrodes and moving the cathode back 0.058 cm.

FACILITY

All performance testing was done in a 1.5 m diameter, 5 m long vacuum facility. The pumping system included four 0.82 m oil diffusion pumps each with a rated capacity of approximately 32 m^3/s at 0.19 Pa. The diffusion pumps were backed by a rotary blower rated at 0.61 m^3/s at 1.3 Pa and two 0.14 m^3/s capacity roughing pumps. The facility was equipped with a displacement type thrust stand described by Haag and Curran[24], accurate to 1%. Calibration was performed *in-situ* under vacuum before and after each test run. Endurance testing was performed in a smaller, bell jar facility pumped by a large mechanical roughing pump which provided background pressures on the order of 100 Pa during arcjet operation.

INSTRUMENTATION AND CALIBRATION

Arcjet power conditioning was provided by a PCU developed by Gruber[25]. Currents were measured using a Hall-effect probe calibrated prior to each test run. Thruster voltages were measured using a commerically available digital multimeter at the power feedthrough to each facility. Propellant flow rates were regulated and measured using thermal conductivity type flow meters. Calibration was performed *in-situ* using a constant volume technique. Flow measurements were accurate to 1%. Facility pressure was measured using ionization gauges in the large facility and with a capacitance manometer in the bell jar. Facility pressures during performance testing were below 0.07 Pa in the large tank and were approximately 140 Pa in the bell jar. Temperatures were measured through quartz windows using a two-color pyrometer with a range of 700-1400°C. Calibration was not made of the temperature readings, and thus the temperature data should not be regarded as absolute but is provided to show trends.

EXPERIMENTAL PROCEDURE

The same performance test sequence was used for all anodes. A scanning electron microscope (SEM) was used to record the condition of each anode before assembly. Each thruster was assembled with a new, sharply-tipped cathode. The propellant used was a 1:2 mixture of nitrogen and hydrogen used to simulate fully decomposed hydrazine. The testing procedure is given in Table I. Not all points were obtained due to a stability problem which was later determined to be caused by a faulty potentiometer on the PCU current level control. Care was taken to minimize unequal starting of the different materials. Ideally each anode should have only been started once during the first performance test; however, due to the faulty control some nozzles experienced up to three starts during the performance test.

After the initial performance test, each nozzle was to be subjected to an 80 hour/single cycle endurance test. The 2% ThO_2/W was the first nozzle tested and, unfortunately, it was the only anode to survive the inital performance test. The endurance test of the 2% ThO_2/W anode was run at a propellant flow rate of 47.6 mg/s and a constant current level of 11 A. After the endurance test, the performance test was repeated using the same testing sequence. SEM micrographs were taken of the 2% ThO_2/W after the second performance test and of the other three nozzles after the first performance test.

RESULTS AND DISCUSSION

2% THORIATED TUNGSTEN

Data showing the inital performance and the performance after a 77 hour endurance test are provided in Table II. The data are presented in the Table in the order which they were taken. Overall efficiency was determined by dividing the thrust power by the input electrical power[18]. It does not include the energy the propellant contains prior to injection to the engine. The inlet pressure was measured near the entrance into the vacuum facility and is provided. There was not a flow limiting orifice in the propellant line, and it is believed that the trends observed in the inlet pressure are similar to those occuring with the arc chamber pressure[26]. Plots of the voltage/current characteristic, the specific impulse versus specific energy, and the efficiency versus specific energy are provided in Figures 2(a), 2(b), and 2(c), respectively. After the endurance test, a voltage increase is noted due to the recession of the cathode tip, similar to that reported by Curran and Haag[6]. At a given specific energy the performance increased slightly over the 77 hour test, most probably due to the decreased anode losses corresponding to the decreased current as the cathode tip receeded. This trend was also noted during the 1000 hour endurance test [6]. Visual observation of the starting and steady-state operation showed no signs of anode material expulsion and a stable plume.

Figure 3(a) and 3(b) are SEM photomicrographs taken before assembly showing the conditions of the converging and diverging sides of the constrictor, respectively. Both images are back scatter electron images (BSE). Machining markings are clearly noted as are small dark deposits. The BSE image is a combination of both topography and chemistry. In general, materials which are heavier will be lighter in contrast; consequently, the dark deposits are not of the same composition as the material and are probably dust particles[27]. Figures 3(c) and 3(d) are the corresponding images taken after the two performance tests and the endurance test. No erosion is evident, only slight melting is noted on the small burrs at the constrictor edge. The low erosion rate is due to the minimal number of starts to which the thruster was subjected. A swirling, starting arc track is noted on the converging side in Figure 3(c) but appears to have caused no damage.

HAFNIUM CARBIDE

The hafnium carbide anode insert failed during inital performance testing. The voltage trace was very steady during start-up and transition to steady-state. The failure occured immediately after decreasing the flow rate to 35.7 mg/s from 47.6 mg/s. After the flow adjustment, the voltage became erratic and the pressure steadily decreased. At that point the test was terminated. As the anode cooled, thermal stresses caused the diverging section of the nozzle to separate from the main section. The fracture occured near the diverging side edge of the constrictor which was probably the area of highest heat flux.

The performance data are presented in Table II. The HfC insert operated at considerably higher temperatures than the 2% ThO_2/W nozzle. The resulting higher propellant chamber pressures caused the thruster to operate at voltages approximately 30 V higher, and the voltage/current characteristic is presented in Figure 2(a). It is not clear why the operating voltage was so much greater. The constrictor diameter is simple to measure, but the determination of the constrictor length is difficult. One possible explanation would be a longer constrictor, due to the difficulty in machining. Another possible explanation for the higher voltage is the much higher arc chamber pressure due to the elevated nozzle temperatures, although the elevated temperatures were unexpected due to the higher emissivity of the HfC over 2% ThO_2/W. With higher operating voltages at a given specific energy level, the anode losses due to the electron current contribution are decreased, and it is expected that the efficiency would increase. The data for the 2% ThO_2/W show an increase in performance after the cathode burned-in the voltage increased. Due to the early failure of the nozzle, it could not be determined if the already high performance exhibited by the HfC insert would have increased after the cathode tip receeded. To determine how the the electronic properties of the material affected performance, the anode inserts should be kept at the same temperature. If the performance gains of the HfC anode over the 2% ThO_2/W were simply due to higher operating temperatures, thermal design should be able to achieve the same results with a pure W or 2% ThO_2/W nozzle. Repetition of the data and expansion of the test envelope are necessary before any conclusions on the performance effects of HfC can be concretely stated. Several attempts were made at producing a second anode insert, but the material shattered during machining.

Figure 4(a) and 4(b) show the inital conditions of the converging and diverging sides, respectively, of the HfC nozzle. The rough, erratic surfaces are testimony to the difficulty in machining the insert. The diverging side edge of the constrictor also had a large burr which is shown in Figure 4(c). The post-test photomicrograph of the converging side is given in Figure 4(d) and shows some throat erosion. Figure 4(e) is a view looking upstream from the diverging side. The fractured surface is visible as is the erosion of the constrictor and several cracks.

One important feature not shown in the SEM images is that a color change was noted on the diverging nozzle surface. The surface had taken on a gold coloration after testing compared to the pre-test dark grey. The nitrogen in the propellant had reacted with the HfC to form HfN which has a gold appearance[28]. Energy Dispersive X-ray (EDX) analysis confirmed the existence of nitrogen in the surface, but also found oxygen. HfC is sometimes formed by exposing HfO_2 to a carbon containing atmosphere and that could be an explanation for some of the oxygen found[28]. It is also possible that the material oxidized during fabrication. Because of the difficulty in fabrication, its susceptibility to thermal stress fracture, and its reactivity to the propellant, hafnium carbide does not appear to be a viable anode material for hydrazine arcjets.

LANTHANUM HEXABORIDE

The lanthanum hexaboride anode insert operated poorly from the inital start up. The exhaust plume was asymmetric and dim, and the voltage never stabilized. Some material ejection was noticed during the 12 min run, and the test was terminated with only one data point obtained. The nozzle fractured a short distance from the diverging edge of the constrictor, the same type of failure as noted with the HfC nozzle. Also, present were many radial cracks and a large gouge on the diverging section, corresponding to the arc attachment region.

The performance data are given Table II, and the single operating point is plotted in Figures 2(a), 2(b), and 2(c) for comparison with the other nozzle inserts. The operating temperature of the LaB_6 anode was the highest of the four nozzles tested. Correspondingly, the voltage of the nozzle is higher than the 2% ThO_2/W, but not as high as the HfC. The efficiency and specific impulse are lower than the control nozzle, showing no performance advantage for the material. The arc attachment point was probably different for this nozzle insert than for the others due to the asymmetry seen in the plume and severe asymmetric erosion of the LaB_6 constrictor. For those two reasons only one data point was obtained, and it is extremely difficult to speculate on the reasons for the performance differences.

The initial conditions of converging and diverging sides of the constrictor are shown in Figures 5(a) and 5(b), respectively. A post-test view of the converging side edge of the constrictor is given in Figure 5(c) and shows the fracturing which occured. A close-up of the surface at the edge of the constrictor is shown in Figure 5(d) and clearly shows formerly molten lanthanum hexaboride. To show the material color variations which resulted during operation a photograph of the fractured surface looking upstream is provided in Figure 5(e). The large eroded area in the diverging section of the nozzle can be seen in the figure as well as a light colored edge. The normally dark purple color of the LaB_6

had turned white surrounded by red and brown in the plane of the fracture near the eroded section. SEM photomicrographs of the area are provided in Figure 5(f) and 5(g). They show severe cracking near the throat and irregular material deposition and melting. Figure 5(f) was taken in BSE and helps to show the different material compositions of the surface. The small, white spots in the bottom and middle of the photomicrograph were identified through EDX as being pure tungsten, which must have come from the cathode. A close-up of one of the spots is shown in Figure 5(g). EDX also revealed the existence of nitrogen in some areas of the diverging section surface. The nitrogen is probably in the form of boron nitride, which may have been caused by chemical reaction with the propellant or erosion of the front insulator. The melting point of LaB_6 and its poor resistance to thermal stress eliminate it as a candidate arcjet anode material.

GRAPHITE

The graphite nozzle successfully completed the initial performance test but was not subjected to an endurance test due to its rapid erosion rate. Throughout the testing the nozzle emitted a steady stream of fine particles, and the voltage fluctuations were severe. The performance data are given in Table II and plotted with the other insert data in Figures 2(a), 2(b), and 2(c). The operating voltages were significantly lower than the thoriated tungsten nozzle due to the increased constrictor diameter caused by erosion during testing; consequently, the chamber pressures and operating voltages were lower than the control.

The initial conditions of the anode are shown in Figures 6(a) and 6(b). Erosion of the converging section near the constrictor is shown in Figure 6(c) which is a secondary electron image (SEI). BSE shows both chemistry and some topography. SEI, on the other hand, shows only topography. From Figure 6(c) it appears that the surface near the constrictor which has eroded is different than that far from the throat. Figures 6(d) and 6(e) are close-ups of the two respective areas and show little difference between the two surfaces when under high magnification. Finally, Figure 6(f) shows the post-test condition of the diverging edge of the constrictor. The most noticable feature is the drastically increased diameter. Because of its severe erosion rates, graphite does not appear to be a good anode material, even for short duration tests.

CONCLUDING REMARKS

Hafnium carbide and lanthanum hexaboride were tested for their viability as anode materials with the hope of increased performance due to lower work functions corresponding to decreased anode losses. Both were respectively identified as the most promising candidates from the carbide and boride families. Both nozzles fractured when subjected to thermal stress and chemically reacted with the propellant. The LaB_6 nozzle also showed signs of melting. Higher performance was noted with the HfC nozzle when compared to the 2% ThO_2/W control anode. The repeatability of the HfC data is uncertain, and the reasons for the higher performance cannot be explained without a larger set of data. Regardless of the performance obtained, the poor resistance to thermal stress and the reactivity of the materials with the propellant limit the use of both materials as hydrazine arcjet anodes.

Graphite was tested with the hope that it would provide a satisfactory material for parametric nozzle tests due to its low material and fabrication costs. The severe erosion rates encountered during testing exclude graphite as an arcjet anode material, even for short duration tests.

REFERENCES

1. Todd, J.P. and Sheets, R.E., "Development of a Regeneratively Cooled 30-kW Arcjet Engine," *AIAA Journal*, Vol. 3, No. 1, pp. 122-126, 1965.

2. John, R.R., "Thirty-Kilowatt Plasmajet Rocket Engine Development," Summary Report on the Second Year Development Program, RAD-TR-64-6, Avco Corp., July 1964, (also NASA CR-54044).

3. Stoner, W.A., "Development of a Plasmajet Rocket Engine for Attitude and Orbit Control," Final Report, FR112-651, Plasmadyne Corp, Santa Ana, CA, June 1964.

4. McCaughey, O.J., *et al.*, "Research and Advanced Development of a 2 kW Arc-Jet Thrustor," Summary Report, Plasmadyne Corp., Santa Ana, CA, June 1964, (also NASA CR-54035).

5. Wallner, L.E. and Czika, J., Jr., "Arc-jet Thrustor for Space Propulsion," NASA TN D-2868, June 1965.

6. Curran, F.M. and Haag, T.W., "An Extended Life and Perfromance Test of a Low-Power Arcjet," AIAA 88-3106, July 1988, (also NASA TM 100942).

7. Smith, W.W., *et al.*, "Low Power Hydrazine Arcjet Flight Qualification," IEPC 91-148, *Proceedings of the 22nd International Electric Propulsion Conference*, October 1991.

8. Haag, T.W. and Curran, F.M., "High-Power Hydrogen Arcjet Performance," AIAA 91-2226, June 1991, (also NASA TM 105143).

9. Hamley, J.A., *et al.*, "10 kW Power Electronics for Hydrogen Arcjets," *Proceedings of the 1992 JANNAF Propulsion Meeting* , February 1992.

10. Sanks, T.M., *et al.*, "The Status and Future Plans for Electric Propulsion Development by the United States Air Force," IEPC 91-006, *Proceedings of the 22nd International Electric Propulsion Conference*, October 1991.

11. Polk, J.E. and Goodfellow, K.D., "Endurance Test of an Ammonia Arcjet at 10 kWe," IEPC-91-068, *Proceedings of the 22nd International Electric Propulsion Conference*, October 1991.

12. Brophy, J., NASA Jet Propulsion Laboratory, Private Communication, January 1992.

13. Hardy, T.L. and Curran, F.M., "Hollow Cathodes in High Pressure Arc Discharges," NASA TM 87098, September 1985.

14. Curran, F.M., *et al.*, "Arcjet Cathode Phenomena," *Proceedings of the 1989 JANNAF Propulsion Meeting* , May 1989, (also NASA TM 102099).

15. Stoner, W.A., "Investigation of a Low-Thrust Plasma Propulsion Device," 1FR-021-1806, Plasmadyne Corp., Santa Ana, CA, February 1961.

16. Sankovic, J.M., *et al.*, "Hydrogen Arcjet Technology," IEPC 91-018, *Proceedings of the 22nd International Electric Propulsion Conference*, October 1991, (also NASA TM 105340).

17. Knowles, S.C., "Arcjet Thruster Research and Technology", Phase I Final Report, Rocket Research Company, Redmond, WA, September 1987, (also NASA CR-182-107).

18. Sankovic, J.M. and Curran, F.M., "Arcjet Thermal Characteristics," AIAA 91-2456 (NASA TM-105156), July 1991.

19. Rieck, G.D., *Tungsten and Its Compunds*, Pergamon Press, 1967, p. 27.

20. Formenko, V.S., *Handbook of Thermionic Properties: Electronic Work Functions and Richardson Constants of Elements and Compounds*, G.V. Samsonov, ed., Plenum Press, 1966.

21. Samsonov, G.V. and Paderno, V.N., "Preparation and Certain Properties of Hafnium Carbide," *J. of Applied Chemistry* (USSR), Vol. 34, No. 5, May 1961, pp. 963-969.

22. "Hot Pressing Data--Lanthanum Hexaboride", CERAC, Inc., 1975.

23. Curran, F.M. and Haag, T.W., "Arcjet Component Conditions Through a Multistart Test," AIAA 87-1060, May 1987, (also NASA TM 89857).

24. Haag, T.W. and Curran, F.M., "Arcjet Starting Reliability: A Multistart Test," AIAA 87-1061, May 1987, (also NASA TM 89867).

25. Gruber, R.P., "Power Electronics for a 1-Kilowatt Arcjet Thruster," AIAA 86-1507, June 1986, (also NASA TM 87340).

26. Talley, K., "Static Pressure Measurements of a Low Power Arcjet," MS Thesis, Air Force Institute of Technology, November 1991.

27. Book, P.O., NASA Lewis Research Center, Private Communication, January 1992.

28. Voitovich, R.F. and Pugach, E.A., "High-Temperature Oxidation of ZrC and HfC," *Powder Metallurgy* (USSR), No. 11, pp. 67-74, November 1973.

ARC CURRENT	FLOW RATE	TIME
A	mg/s	min
ARC IGNITION		
11	47.6	30
10	47.6	15
9	47.6	15
8	47.6	15
7	47.6	15
10	35.7	30
9	35.7	15
8	35.7	15
7	35.7	15
6	35.7	15
ARC EXTINCTION		

TABLE I - PERFORMANCE TEST PROCEDURE

MATERIAL	CURRENT	VOLTAGE	POWER	THRUST	FLOW RATE	SPECIFIC ENERGY	SPECIFIC IMPULSE	EFFICIENCY	INLET PRESSURE	TEMPERATURE
	A	V	W	mN	mg/s	MJ/kg	s		kPa	°C
2% ThO2/W	0.0	0.0	0	55.3	47.6		118		182	
(Initial)	0.0	0.0	0	41.1	35.7		117		134	
	11.0	89.4	983	183	47.6	20.7	392	0.359	353	872
	10.0	91.7	917	178	47.6	19.3	382	0.364	347	835
	9.0	93.9	845	172	47.6	17.8	368	0.368	339	785
	8.0	96.9	775	166	47.6	16.3	355	0.373	330	<700
	10.0	82.4	824	142	35.7	23.1	406	0.344	276	875
	9.0	85.9	773	138	35.7	21.7	395	0.347	272	849
2% ThO2/W	0.0	0.0	0	54.4	47.6		117		182	
After 77 h	0.0	0.0	0	40.4	35.7		115		134	
	11.0	97.6	1074	195	47.6	22.6	418	0.374	372	917
	10.0	99.1	991	187	47.6	20.8	402	0.374	362	874
	9.0	102.8	925	182	47.6	19.4	390	0.376	355	842
	8.0	103.7	830	172	47.6	17.4	369	0.375	340	<700
	10.0	89.0	890	148	35.7	24.9	425	0.349	292	962
	9.0	90.8	817	142	35.7	22.9	408	0.350	283	901
	11.0	96.9	1066	194	47.6	22.4	417	0.373	372	923
	10.0	99.2	992	187	47.6	20.8	401	0.372	364	878
HfC	0.0	0.0	0	54.9	47.6		118		183	
	0.0	0.0	0	40.7	35.7		116		137	
	11.0	119.0	1309	217	47.6	27.5	465	0.378	448	1074
	10.0	122.0	1220	209	47.6	25.6	449	0.379	440	1014
	9.0	125.2	1127	202	47.6	23.7	433	0.380	429	971
	8.0	129.4	1035	195	47.6	21.7	418	0.386	417	924
	10.0	104.7	1047	155	35.7	29.3	445	0.325	367	1080
LaB6	0.0	0.0	0	54.3	47.6		116		178	
	0.0	0.0	0	40.4	35.7		115		133	
	11.0	102.5	1128	187	47.6	23.7	401	0.327	369	1151
C	0.0	0.0	0	55.2	47.6		118		187	
	0.0	0.0	0	40.9	35.7		117		140	
	11.0	85.3	938	169	47.6	19.7	363	0.322	291	933
	10.0	85.5	855	161	47.6	18.0	347	0.322	255	872
	9.0	86.2	776	153	47.6	16.3	328	0.318	227	827
	8.0	94.1	753	150	47.6	15.8	322	0.315	202	795
	10.0	76.7	767	120	35.7	21.5	345	0.266	164	954
	9.0	77.7	699	116	35.7	19.6	332	0.271	161	916

TABLE II - PERFORMANCE DATA

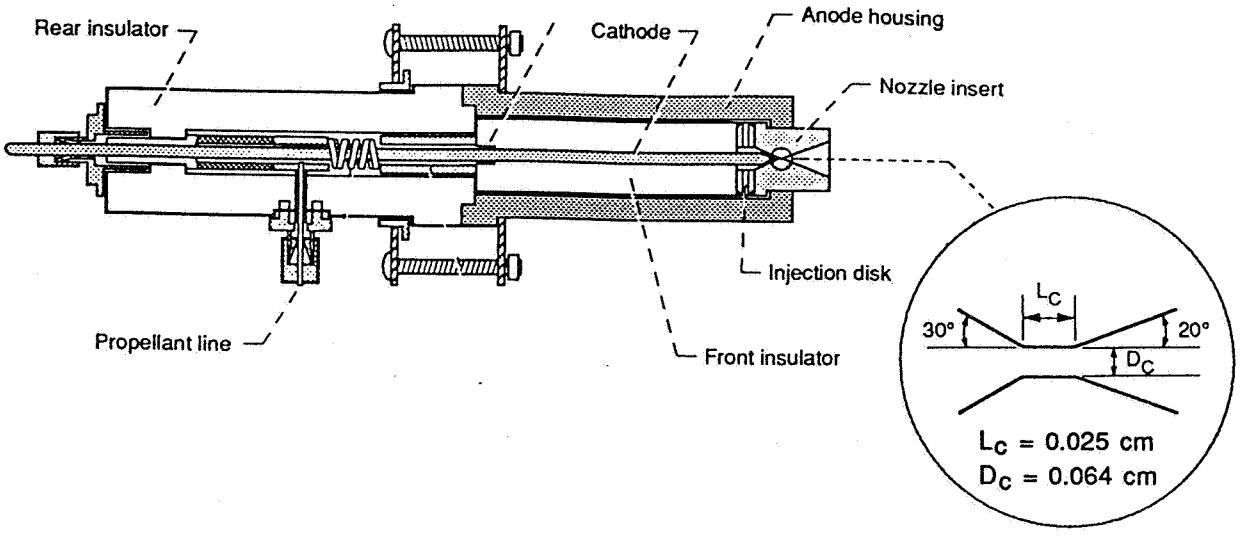

FIGURE 1 - CROSS-SECTIONAL SCHEMATIC OF MODULAR ARCJET THRUSTER

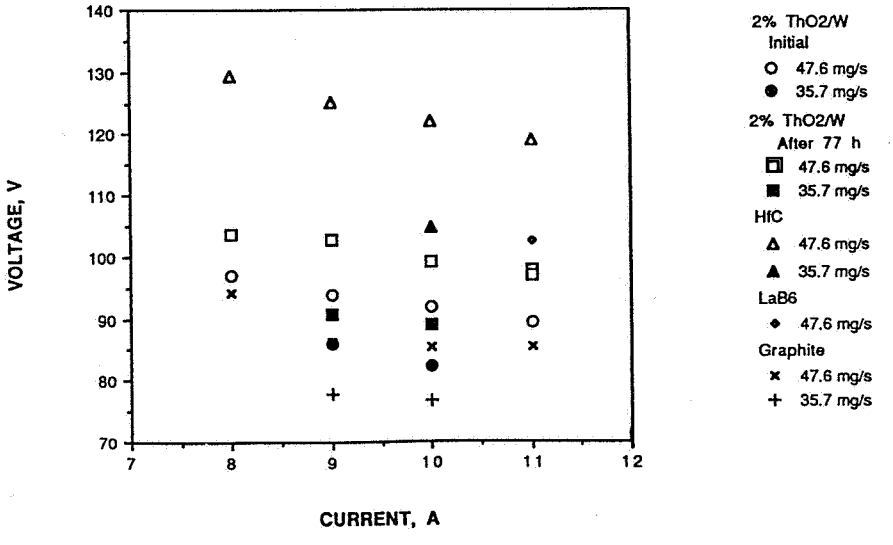

(A) VOLTAGE-CURRENT CHARACTERISTICS

FIGURE 2 - (CONTINUED).

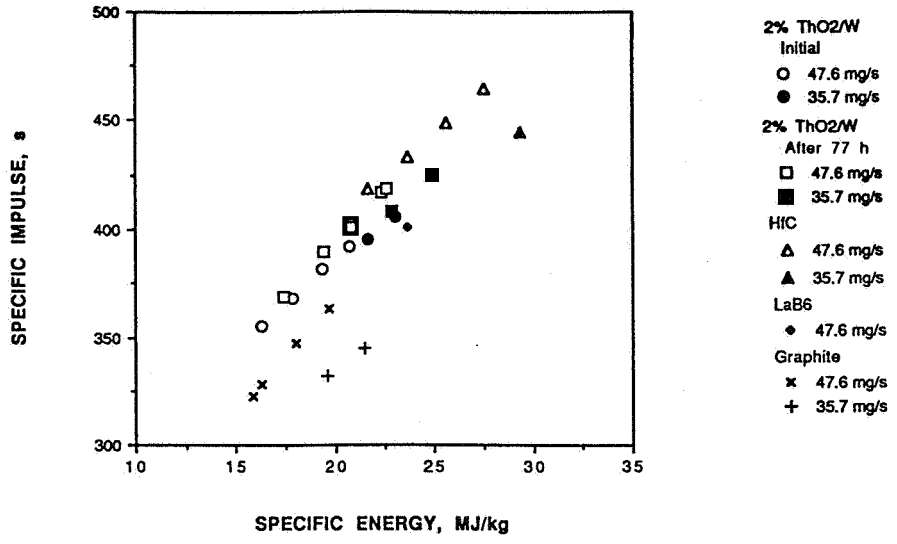

(B) SPECIFIC IMPULSE VERSUS SPECIFIC ENERGY

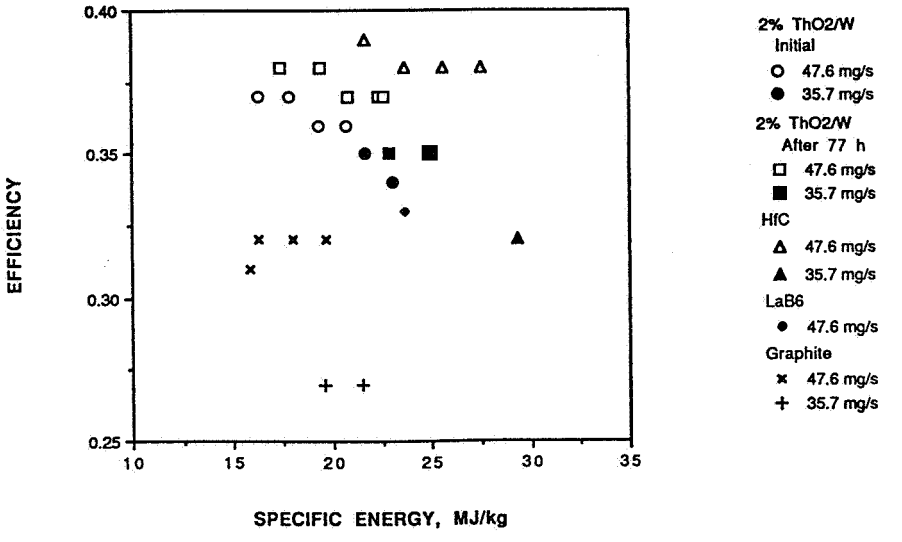

(C) EFFICIENCY VERSUS SPECIFIC ENERGY

FIGURE 2 - PERFORMANCE CHARACTERISTICS

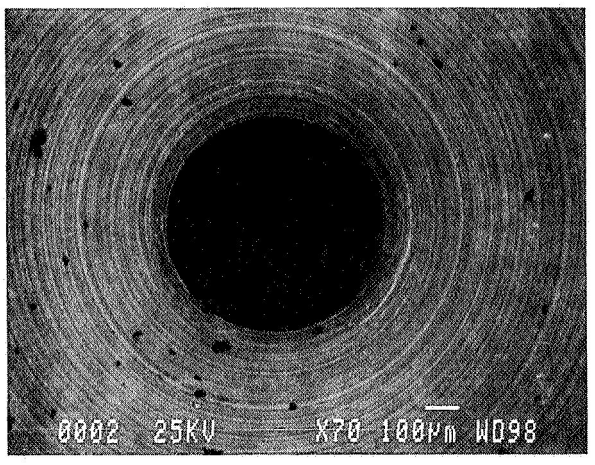

(a) Converging side before testing, SEM BSE image (70x).

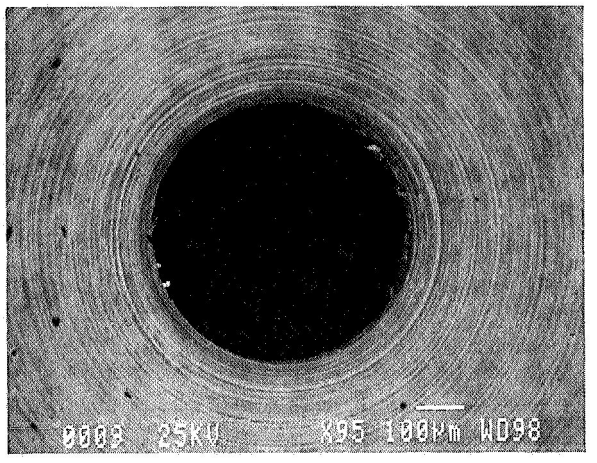

(b) Diverging side before testing, SEM BSE image (95x).

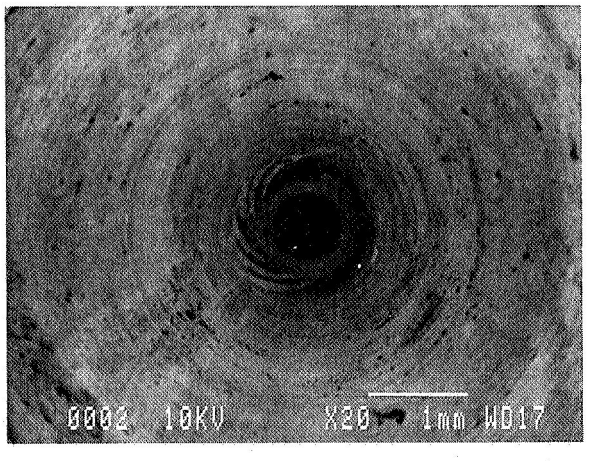

(c) Converging side after 77 hr test, SEM BSE image (20x).

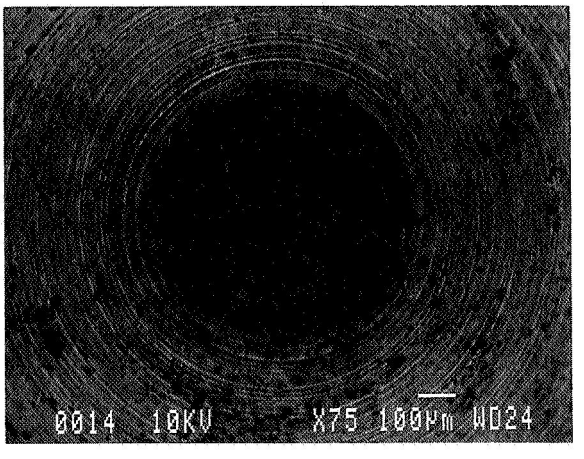

(d) Diverging side after 77 hr test, SEM BSE image (75x).

Figure 3.—Two percent thoriated tungsten anode insert.

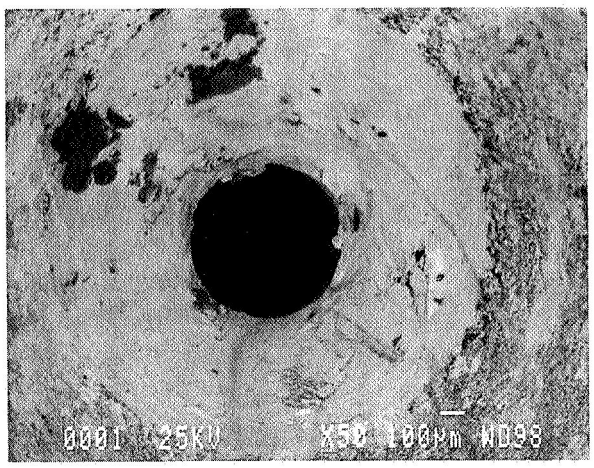

(a) Converging side before testing, SEM BSE image (50x).

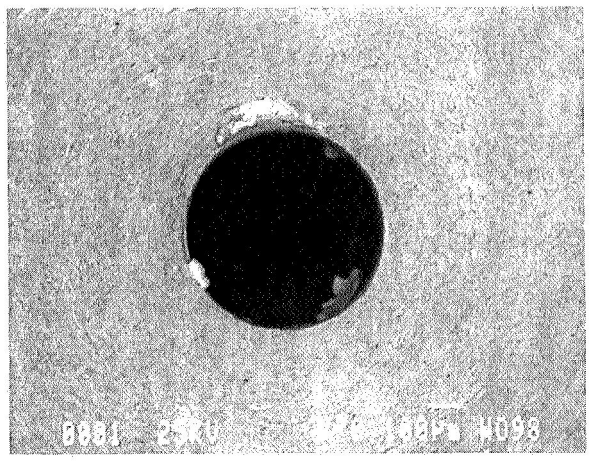

(b) Diverging side before testing, SEM BSE image (70x).

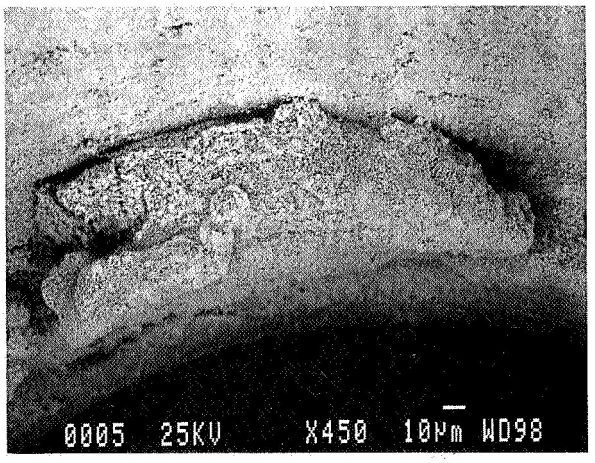

(c) Close-up of constrictor diverging side edge before testing, SEM SEI image (450x).

(d) Converging side after initial performance test, SEM SEI image (50x).

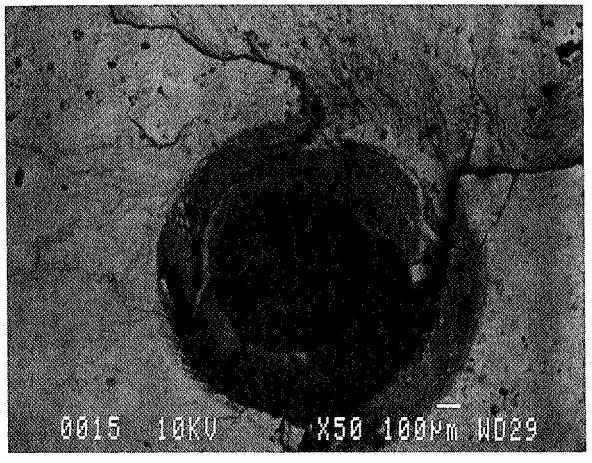

(e) Diverging side after initial performance test, SEM BSE image (50x).

Figure 4.—Hafnium carbide anode insert.

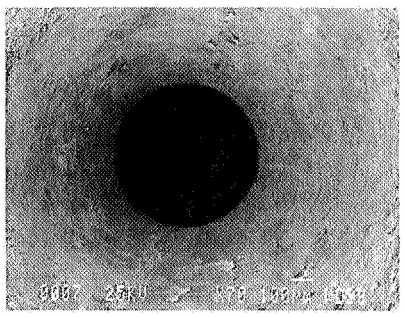

(a) Converging side before testing, SEM SEI image (70x).

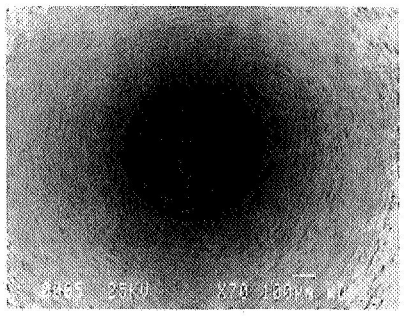

(b) Diverging side before testing, SEM SEI image (70x).

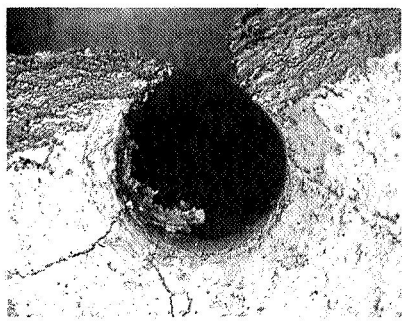

(c) Converging side after initial performance test, SEM BSE image (75x).

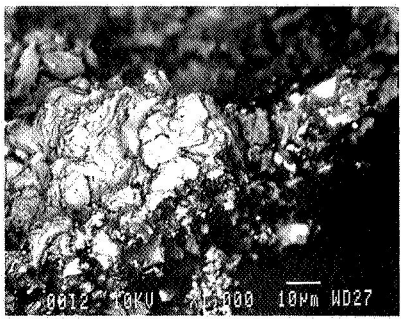

(d) Close-up of converging side constrictor edge after initial performance test, SEM SEI image (1000x).

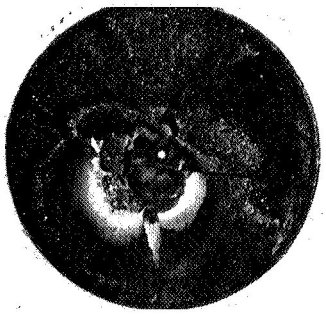

(e) Photograph of fractured anode insert with view upstream after initial performance test.

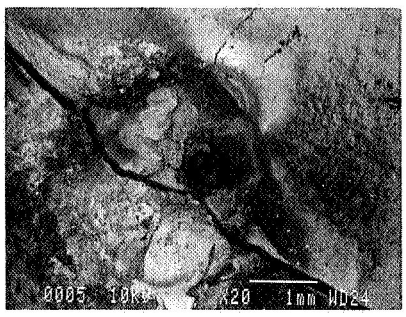

(f) Diverging side after initial performance test, SEM BSE image (20x).

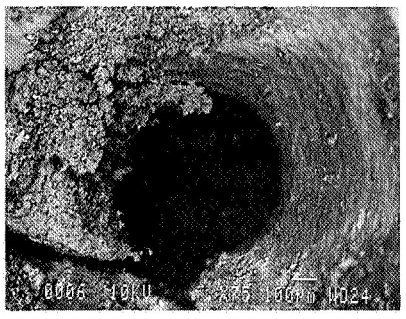

(g) Close-up of diverging side constrictor edge after initial performance test, SEM BSE image (75x).

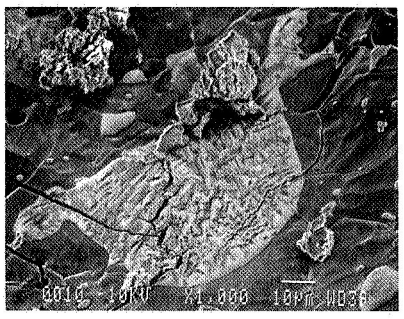

(h) Tungsten deposit on diverging side of anode after initial performance test, SEM BSE image (1000x).

Figure 5.—Lanthanum hexaboride anode insert.

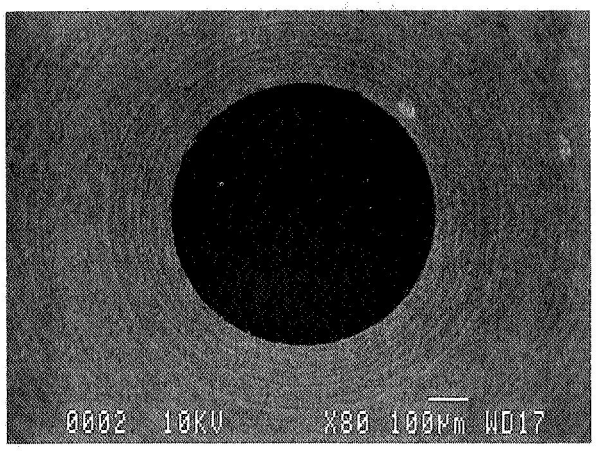

(a) Converging side before testing, SEM BSE image (80x).

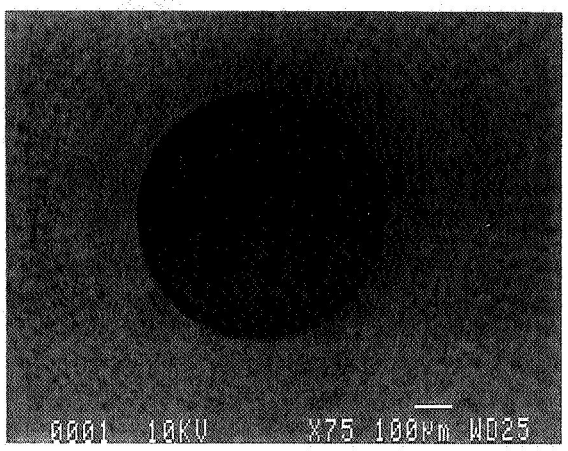

(b) Diverging side before testing, SEM SEI image (75x).

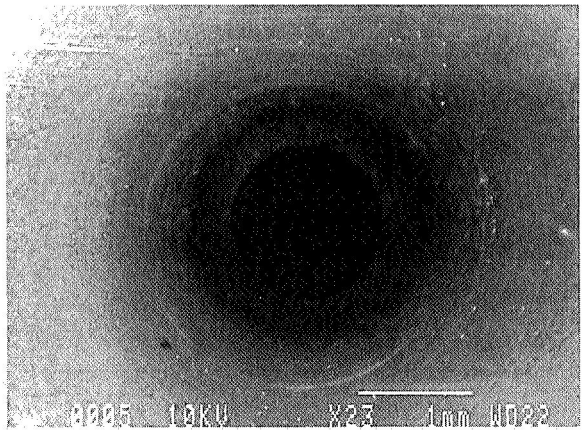

(c) Converging side after initial performance test, SEM SEI image (23x).

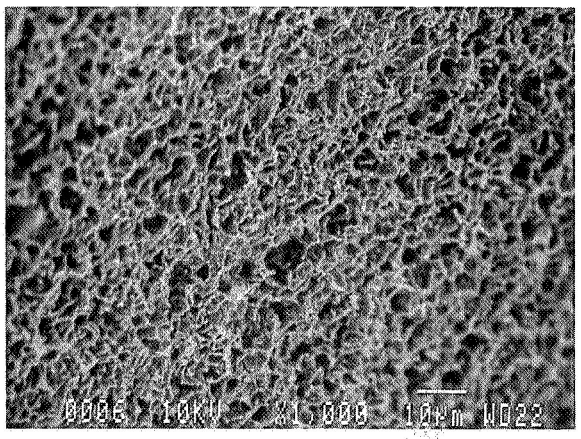

(d) Close-up of converging side surface near constrictor edge after initial performance test, SEM SEI image (1000x).

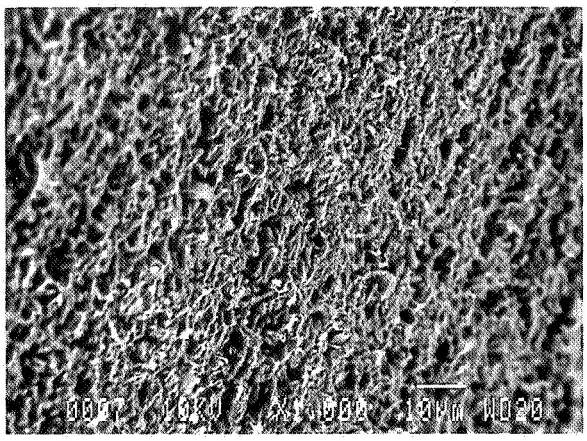

(e) Close-up of converging side surface far from constrictor edge after initial performance test, SEM BSE image (1000x).

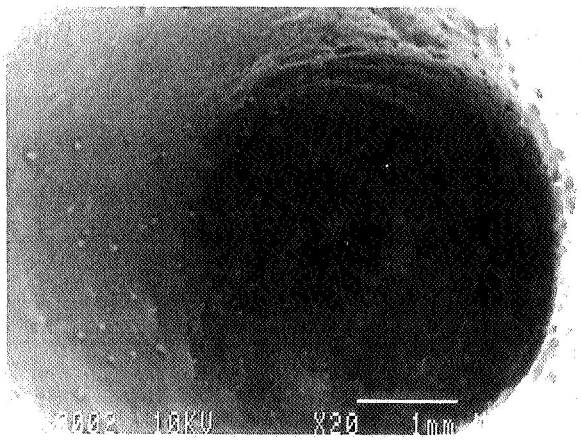

(f) Diverging side after initial performance test, SEM BSE image (20x).

Figure 6.—Graphite anode insert.

REPORT DOCUMENTATION PAGE

Form Approved
OMB No. 0704-0188

1. AGENCY USE ONLY (*Leave blank*)	2. REPORT DATE	3. REPORT TYPE AND DATES COVERED
		Technical Memorandum

4. TITLE AND SUBTITLE

Effects of Anode Material on Arcjet Performance

5. FUNDING NUMBERS

WU–506–42–31

6. AUTHOR(S)

John M. Sankovic, Frank M. Curran, and C.A. Larson

7. PERFORMING ORGANIZATION NAME(S) AND ADDRESS(ES)

National Aeronautics and Space Administration
Lewis Research Center
Cleveland, Ohio 44135–3191

8. PERFORMING ORGANIZATION REPORT NUMBER

E–6873

9. SPONSORING/MONITORING AGENCY NAMES(S) AND ADDRESS(ES)

National Aeronautics and Space Administration
Washington, D.C. 20546–0001

10. SPONSORING/MONITORING AGENCY REPORT NUMBER

NASA TM–105799

11. SUPPLEMENTARY NOTES

Prepared for the 1992 JANNAF Propulsion Meeting, Indianapolis, Indiana, February 24–28, 1992. John M. Sankovic and Frank M. Curran, NASA Lewis Research Center. C.A. Larson, United States Air Force Academy, Colorado Springs, Colorado. Responsible person, John M. Sankovic, (216) 977–7429.

12a. DISTRIBUTION/AVAILABILITY STATEMENT

Unclassified - Unlimited
Subject Category 20

12b. DISTRIBUTION CODE

13. ABSTRACT ***(Maximum 200 words)***

Anodes fabricated from four different materials were tested in a modular arcjet thruster at 1 kW power level on nitrogen/hydrogen mixtures. A two-percent thoriated tungsten anode served as the control. Graphite was chosen for its ease in fabrication, but experienced severe erosion in the constrictor and diverging side. Hafnium carbide and lanthanum hexaboride were chosen for their low work functions but failed due to thermal stress and reacted with the propellant. When compared to the thoriated tungsten nozzle, thruster performance was significantly lower for the lanthanum hexaboride insert and the graphite nozzle, but was slightly higher for the hafnium carbide nozzle. Both the lanthanum hexaboride and hafnium carbide nozzle operated at higher voltages. An attempt was made to duplicate higher performance hafnium carbide results, but repeated attempts at machining a second anode insert were unsuccessful. Graphite, hafnium carbide, and lanthanum hexaboride do not appear viable anode materials for low power arcjet thrusters.

14. SUBJECT TERMS

Arcjet thruster; Anode electrodes; Materials

15. NUMBER OF PAGES

14

16. PRICE CODE

A03

17. SECURITY CLASSIFICATION OF REPORT	18. SECURITY CLASSIFICATION OF THIS PAGE	19. SECURITY CLASSIFICATION OF ABSTRACT	20. LIMITATION OF ABSTRACT
Unclassified	Unclassified	Unclassified	